Biosensors and Bioelectronics 288 (2025) 117815

Contents lists available at ScienceDirect

Biosensors and Bioelectronics

journal homepage: www.elsevier.com/locate/bios

Negative pressure-controlled microneedle-microfluidic hybrid chip for painless in situ detection of ovalbumin-sIgE in skin interstitial fluid

Jun Zhang [a], Huiting Lian [a,b], Guangming Liu [c,e], Qingmei Liu [c], Bin Liu [a,b,d,*], Xiaofeng Wei [a,b,d,**]

[a] College of Materials Science and Engineering, Huaqiao University, Xiamen, 361021, China
[b] Key Laboratory of Molecular Designing and Green Conversions, Huaqiao University, Xiamen, 361021, China
[c] College of Ocean Food and Biological Engineering, Jimei University, Xiamen, 361021, China
[d] Xiamen Key Laboratory of Optoelectronic Materials and Advanced Manufacturing, Huaqiao University, Xiamen, 361021, China
[e] College of Marine Biology, Xiamen Ocean Vocational College, Xiamen, 361100, Fujian, China

ARTICLE INFO

Keywords:
Food allergy
Ovalbumin
Specific IgE
Interstitial skin fluid
Microneedle
Painless detection

ABSTRACT

Allergen-specific immunoglobulin E (IgE) is a gold marker for the diagnosis of food allergy. The existing traditional diagnostic methods not only require blood collection and separation by professionals, but also are not friendly to pain-sensitive patients such as infants. Skin interstitial fluid (ISF) is highly similar to serum components, but its clinical value in the diagnosis of food allergy as an excellent sample for in situ painless detection is still unclear. To address the above issues, gel microneedles, functionalized paper-based modification and microfluidic technology were used to create an ISF integrated collection and detection device (ISF-ICD) for mouse ovalbumin (OVA)-sIgE. With the classical OVA-allergy model mice, the effects of ISF-ICD and traditional blistering method on collecting ISF were compared and analyzed, and the detection accuracy was compared with the traditional serum ELISA test results to further explore the relationship between ISF and serum OVA-sIgE content and changes. The results showed that the minimum detection limit of OVA-sIgE in ISF detected by the ISF-ICD was 0.064 ng/mL. The content of OVA-sIgE in ISF of OVA-allergic mice measured by ISF-ICD was similar to blister method. At 30 min after challenge, the OVA-sIgE content in ISF of OVA-allergic mice measured by different collection methods were 77.49 ± 9.11 ng/mL (ISF-ICD method) and 89.82 ± 11.26 ng/mL (blister method), respectively, which was about 1/15 of the serum OVA-sIgE content (1551.33 ± 30.51 ng/mL) measured by ELISA. In summary, the ISF-ICD has great significance to realize the screening and diagnosis of painless allergens for the prevention and treatment of food allergy.

1. Introduction

Food allergy is a major public health issue globally, affecting about 8 % of children and 10 % of adults (Sampath et al., 2021). Food allergy has a negative impact on the lives of patients with allergy and their families, and there is no curative treatment (Gupta et al., 2018). At present, the most effective clinical treatment for food allergy is to avoid allergens, or timely drug intervention in the early stage of allergy to achieve the purpose of relieving allergic symptoms and relieving pain for patients (Dantzer and Kim, 2024). Therefore, it is very important for the screening of allergens and the monitoring of early markers of allergic reactions in patients with food allergy. It also has great clinical significance for the rescue and symptomatic treatment of patients with food allergy.

Both new tests (eg, the basophil activation test) and improved optimization of information provided by existing tests (eg, the skin prick test and measurement of serum specific immunoglobulin E (sIgE) level) can contribute to improving the accuracy of food allergy diagnosis (Bartha et al., 2024). However, Fragile veins not only increase the difficulty of blood collection, but also require qualified professional medical personnel to operate. Blood collection is usually invasive, which can easily lead to wound infection and cause certain physiological damage and psychological shadow to pain-sensitive people, such as infants (Wei et al., 2024). Although the skin prick test does not need to collect blood,

* Corresponding author. College of Materials Science and Engineering, Huaqiao University, Xiamen, 361021, China
** Corresponding author. College of Materials Science and Engineering, Huaqiao University, Xiamen, 361021, China
E-mail addresses: bliu@hqu.edu.cn (B. Liu), xfwei@hqu.edu.cn (X. Wei).

https://doi.org/10.1016/j.bios.2025.117815
Received 3 April 2025; Received in revised form 7 July 2025; Accepted 22 July 2025
Available online 22 July 2025
0956-5663/© 2025 Published by Elsevier B.V.

the allergen needs to enter the subcutaneous tissue directly with the help of a pricking needle, and skin symptoms caused by allergies will occur at the pricking site, which may lead to serious allergic reactions, it usually needs to be observed by qualified medical institutions and authoritative medical personnel (Sicherer and Sampson, 2018). Therefore, it is of great practical significance to find a sensing mechanism of allergic markers that can replace serological detection.

In disease diagnosis and detection, interstitial fluid (ISF) is regarded as a substitute for blood (Li et al., 2024). Since the skin is relatively easy to access and contains a large amount of ISF, ISF plays an important role in the diagnosis of medical diseases, especially in the diagnosis of diseases with skin symptoms (Friedel et al., 2023). Studies have shown that the protein concentration in ISF is conserved relative to serum, and almost all proteins present in serum can be detected in ISF. ISF can be collected from the skin through blisters. This method requires the skin to be absorbed for at least 30 min to obtain blisters full of ISF (Lundberg et al., 2013). Time-consuming, high risk, and the need for medical expertise and professional equipment limit the use of ISF in the field of disease diagnosis. With the continuous development of science and technology, the microneedle (MN) collecting ISF is considered to be a promising ISF extraction method (Eltayib et al., 2016; Kolluru et al., 2019; Min et al., 2021). The length of the MN is usually less than 1 mm, and the tip is much sharper than the subcutaneous injection needle. Such a geometric design allows the MN to effectively penetrate the stratum corneum and form microscale ISF extraction channels without touching blood vessels, nerve fibers, or skin or dermal endings (Zhu et al., 2020). Due to its small size and short penetration depth, MNs are endowed with painless, simple and minimally invasive ability to collect skin ISF. Many studies have reported that MNs can collect ISF painlessly and show great advantages in the field of disease diagnosis (Li et al., 2022; Takeuchi et al., 2022). As reported, during the skin prick test, allergens are transmitted subcutaneously using a prick needle and bind to sIgE on the surface of subcutaneous mast cells, causing mast cells to degranulate. Then, allergic symptoms appear at the prick site to determine the specific allergen involved in the patient (Boyd and Santos, 2025; Foong et al., 2021; Popov et al., 2020). However, whether there is sIgE in ISF, the concentration relationship between sIgE in ISF and sIgE in serum, and whether sIgE in ISF has clinical significance in the field of food allergy diagnosis have not been clearly reported.

In this study, ovalbumin (OVA)-induced food allergy was used as a model system. The classic OVA food allergy mouse model was established, and a self-designed integrated microfluidic chip for ISF collection and detection, combined with a negative pressure valve switch, was employed to achieve segmented control of the entire process. It is named interstitial fluid integrated collection and detection device (ISF-ICD). This approach aims to enable the quantitative detection of OVA-sIgE levels in mouse ISF. The results obtained from the chip-based detection method were compared with those from the conventional serum ELISA assay. This comparison elucidated the relationship between the concentration and dynamic changes of sIgE in mouse ISF and serum, providing a theoretical foundation and data support for the development of a painless, real-time detection method for allergen sIgE in ISF.

2. Experimental section

The details demonstrate in the supplementary material.

3. Results and discussions

3.1. Preliminary validation of OVA-sIgE in mouse ISF

The clinical use of allergen skin patch test is to cause local allergic reaction of the patient's skin through specific allergen preparations, and to determine whether the patient is allergic to the allergen through allergic symptoms. This indicates that the ISF of allergic patients is likely to contain sIgE. Thus, as shown in Fig. 1A, the mouse OVA-sIgE was injected into the tail vein of normal mice. Four hours later, the ISF of the mice was collected by blister aspiration through the blistering tool (Fig. 1B and C), and the whole blood was collected from the posterior plexus of the mice and the serum was separated. The content of OVA-sIgE in serum and ISF was determined using a commercial ELISA kit. The standard working curve is shown in Fig. 1D. The ELISA results in serum and ISF were shown in Fig. 1E. The concentration of OVA-sIgE in mouse serum was 1892.52 ± 96.48 ng/mL, while the concentration of OVA-sIgE in ISF was 139.87 ± 9.01 ng/mL.

This result indicates that IgE is really present in ISF and derived from serum. Our results were similar to the results obtained by Maria T. Arévalo et al. using shotgun quantitative proteomics, which proved the presence of IgE in ISF (Tran et al., 2018). Notably, the IgE concentration in interstitial fluid (ISF) was significantly lower than that in serum ($p < 0.05$). This observed discrepancy became the focus of subsequent mechanistic investigations.

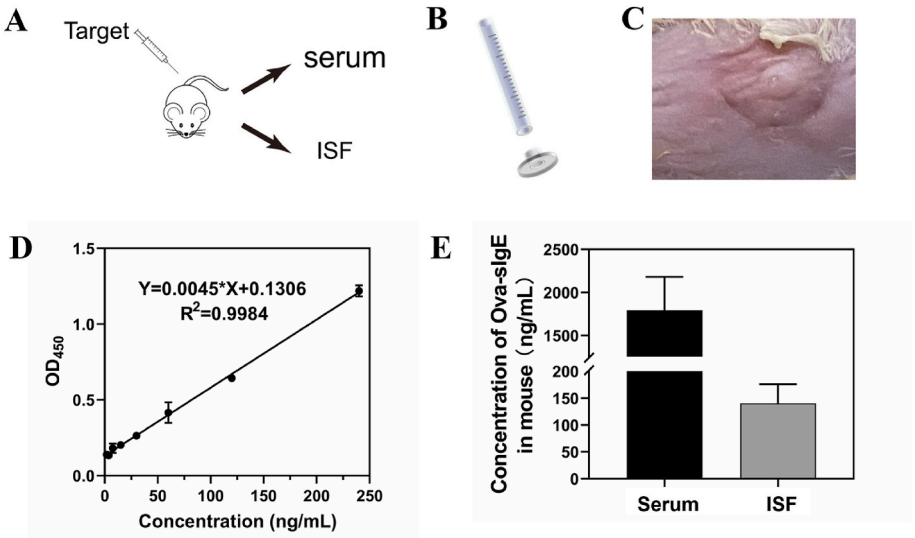


Fig. 1. (A) Schematic diagram of establishing a simple animal model using the tail vein standard addition method. **(B)** The tool for pumping blisters used in blistering method. **(C)** The actual effect of suction blisters on the skin surface of mice. **(D)** Standard working curve of commercial mouse OVA-sIgE ELISA kits. **(E)** Comparison of OVA-sIgE content in serum and ISF of mice injected with standard substances through tail vein (n = 5).

3.2. Fabrication and morphological characterization of GelMA MNs

Subsequently, we began to prepare MNs for non-invasive collection of ISF. The design scheme of MN and the specifications of the die are shown in Fig. 2A–B. The cross-linking of Gelatin and MA was proved by NMR spectroscopy (Fig. S1A–B). The ninhydrin colorimetric method proved that GelMA with an amino substitution degree of 69.5 % was successfully prepared (Fig. S1C), this is similar to the results of Zhu et al., (2020). The physical image of the PMMA microneedle mold manufactured by the laser engraving machine is shown in Fig. 2C, and the observation results under the optical microscope are shown in Fig. 2D–E. The prepared microneedles are shown in Fig. 2F, and the results observed under an optical microscope are shown in Fig. 2G–H. The microstructure of the microneedles was further characterized by scanning electron microscopy. It was observed that the microneedles were inverted conical shape, with smooth surface, uniform size, neat array distribution, and tip length of about 600 μm and tip diameter of about 10 μm (Fig. 2I–K).

3.3. Optimization and performance characterization of GelMA MNs

In order to make GelMA have good hygroscopicity and mechanical strength in the process of skin puncture to collect ISF, we optimized GelMA concentration and Crosslinking time. As shown in Fig. 3A–B, the moisture absorption rate of GelMA MN decreased with the increase of GelMA concentration in same time, and it was 225.79 %–79.73 % in the range of 15 %–35 % concentration. This is because after photo cross-linking, the low concentration of MN has loose internal molecules and weak structural strength, which is conducive to the entry of water molecules, while the high concentration of MN has tight internal

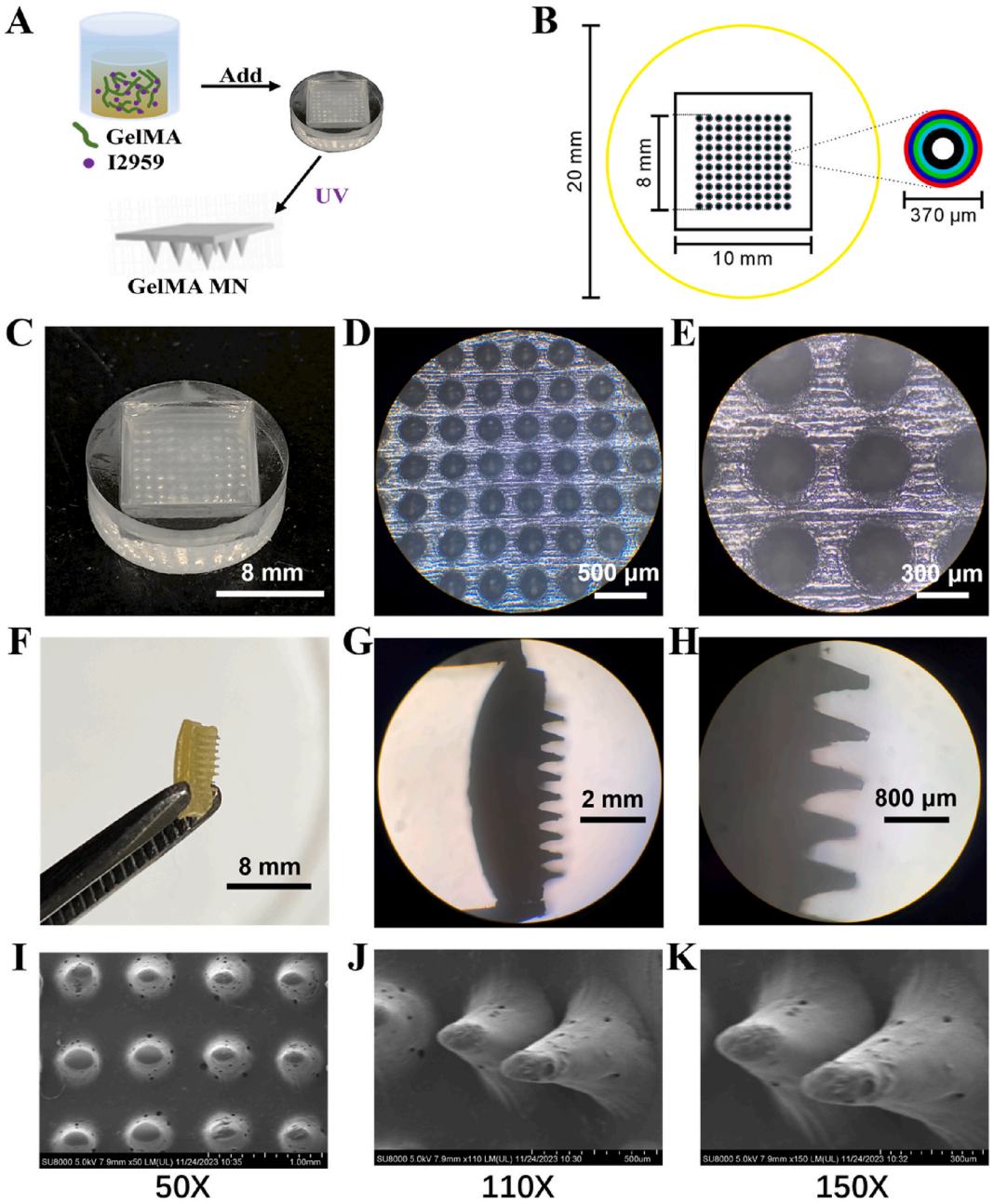


Fig. 2. (A) The schematic diagram of microneedle preparation steps. **(B)** Laser engraving design of microneedle mold. Mold physical map **(C)** and microscopic observation results under different magnifications **(D, E)**. Microneedle physical map **(F)** and microscopic observation results at different magnifications **(G, H)**. Scanning electron microscopy of microneedles at different magnifications **(I–K)**.

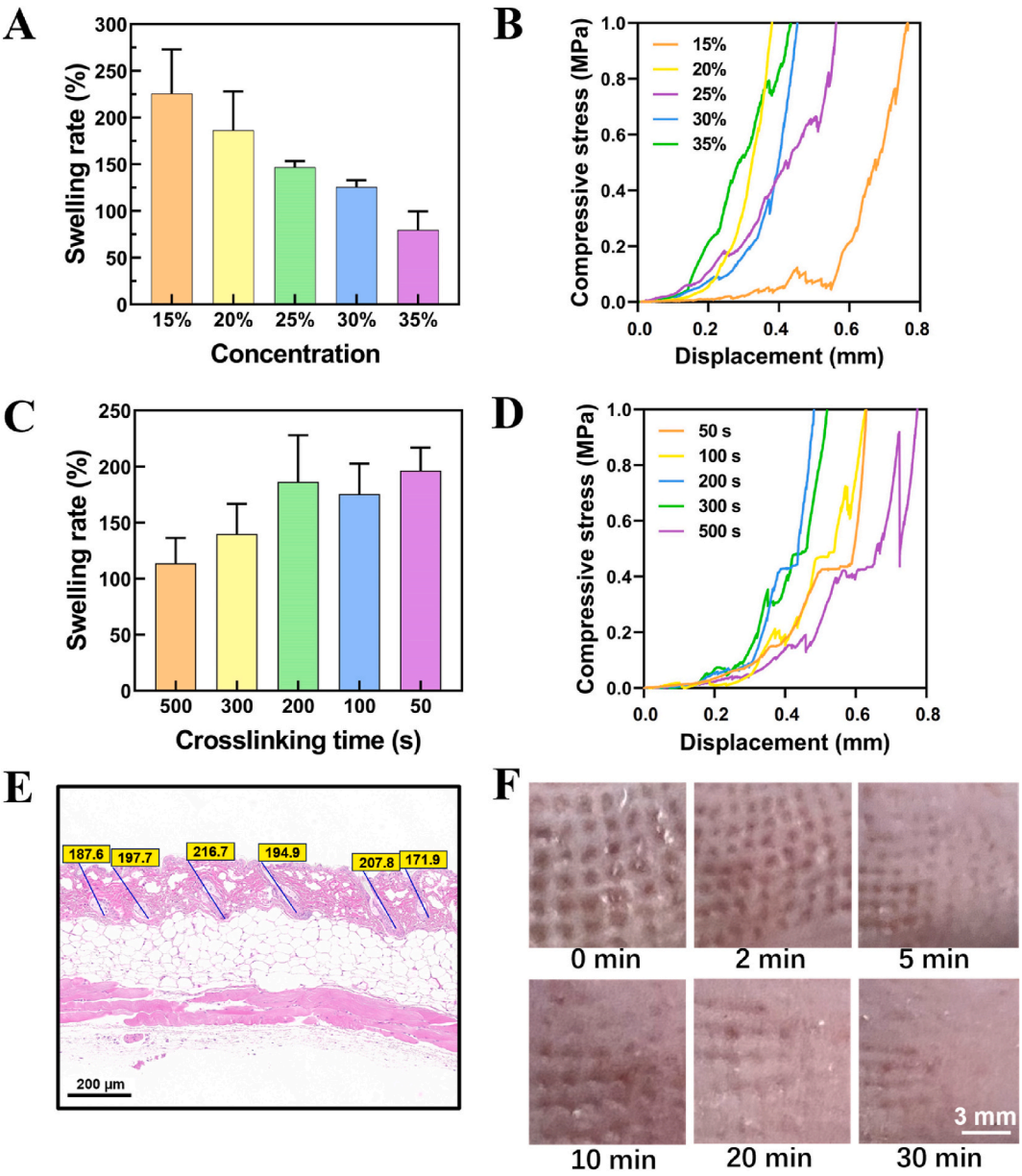


Fig. 3. Characterization of various Microneedle. The swelling rate **(A)** and stress-strain curve **(B)** of microneedles with different GelMA concentrations (n = 5). The swelling rate **(C)** and stress-strain curve **(D)** of microneedles under different crosslinking time (n = 5). **(E)** H&E staining results of mouse skin after microneedle invasion. **(F)** The recovery of mouse skin after microneedle invasion.

molecules and high structural strength, which is not conducive to the entry of water molecules, which is similar to the properties of most gelatin (Bigi et al. 2001, 2002; Cao et al., 2007). As shown in Fig. 3C–D, the moisture absorption rate was 113.82 %–196.47 % in the concentration range of photo crosslinking 50 s–500 s. The longer the photo crosslinking time, the lower the moisture absorption rate of GelMA MN. This is because the longer the photo crosslinking time, the closer the connection between GelMA molecules, and the less easy for water molecules to enter, and vice versa. And too long photo crosslinking will lead to an increase in brittleness of GelMA MN, which is easier to break in mechanical stress tests. Combining the two key factors of moisture absorption rate and mechanical strength, when the concentration of GelMA is 25 % and the photo crosslinking time is 200 s, the deformation of the microneedles was about 0.3 mm at about 0.6 MPa (Fig. S2), which met the strength of the penetrating skin tissue described in the literature (Yuan et al., 2021; Zhang et al., 2024). The optimized microneedle has good water absorption (Fig. S3A), At a stable 30 μL/200 s absorption rate, we obtained ~135 μL ISF per 15 min collection. After freeze-drying of the used microneedle, the SEM results show that the microneedle tip only slightly blunted and no obvious fracture occurred (Fig. S3B–C).

We prepared GelMA MN according to the optimized conditions and used it for in vivo mouse ISF collection. The mouse skin after GelMA MN invasion was stained with HE. The results are shown in Fig. 3E. The microneedles successfully penetrated the stratum corneum to the ISF aggregation layer, and the invasion depth was about 200 μm. And the skin wound after microneedle invasion can be basically restored in about 30 min (Fig. 3F). So far, we have successfully prepared GelMA MNs that can be used for painless and minimally invasive collection of ISF in mice.

3.4. Functionalization of paper-based substrates for OVA-sIgE detection

As shown in Fig. 4A, chitosan, OVA and BSA were uniformly dropped on the surface of the paper chip in turn. After drying, a functionalized

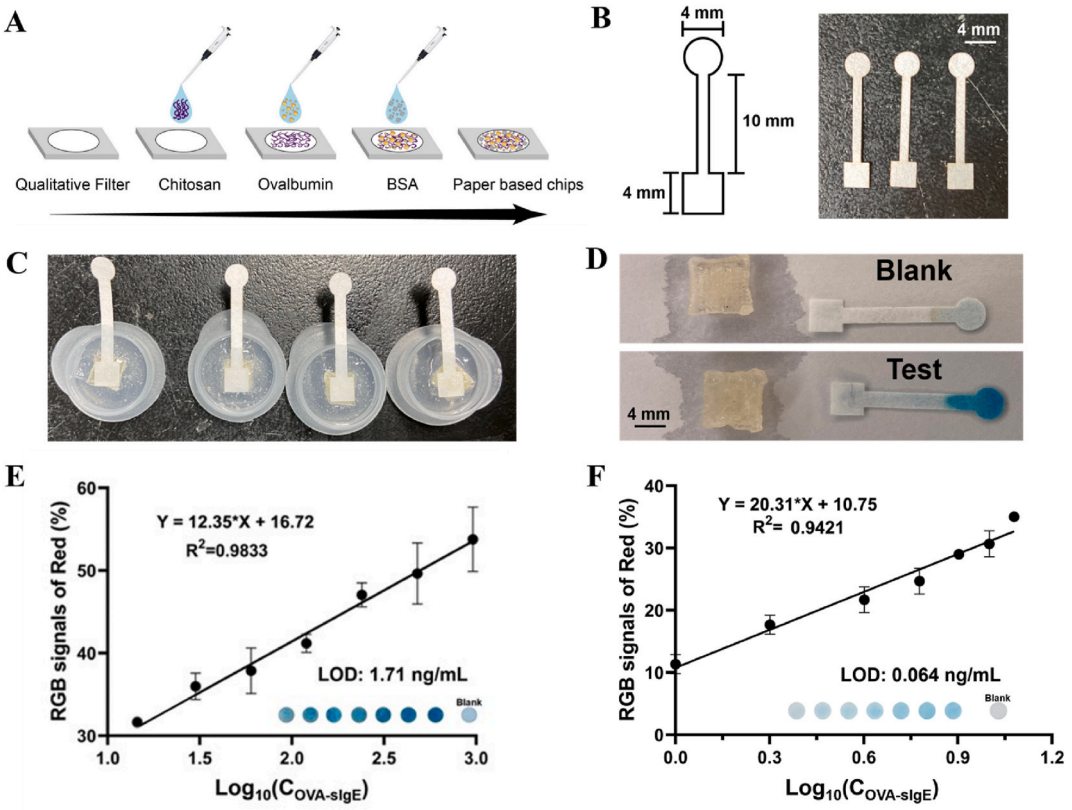


Fig. 4. (A) Functional modification schematic of paper-based chip. **(B)** Functional paper-based chip design and physical map. **(C)** The schematic diagram of microneedle-paper-based chip combined collection of gel to simulate skin ISF. **(D)** Feasibility test of OVA-sIgE in gel-simulated skin by microneedle-paper chip. The standard working curves of the paper-based detection chip area adapted to high OVA-sIgE levels **(E)** and low OVA-sIgE levels**(F).**

paper base capable of specifically recognizing OVA-sIgE was obtained. The improved paper substrate is shown in Fig. 4B. The circular end is the detection area, and the connection channel between the square end and the middle is the transmission area of the microneedle collecting ISF. As shown in Fig. 4C, when the ISF is collected into the microneedle, the paper base will further transmit the ISF to the circular detection area for the next detection of the target. Then, we established a classical paper-based color sensing system using mouse OVA-sIgE standard, HRP-anti-mouse OVA-sIgE, and TMB. The color value can be read by the mobile phone RGB software to calculate the content of OVA-sIgE. The whole process does not require the support of professional spectral equipment such as microplate readers. As shown in Fig. 4D, by verifying on the gel simulated skin containing mouse OVA-sIgE, the functionalized paper-based chip can well realize the visual detection of OVA-sIgE. By further optimizing the concentration of HRP-anti-mouse OVA-sIgE, we established two working curves greater than 15 ng/mL (15–960 ng/mL, $Y = 12.35*X+16.72$, $R^2 = 0.9833$) and less than 15 ng/mL (1–15 ng/mL, $Y = 20.31*X+10.75$, $R^2 = 0.9421$) to adapt to different OVA-sIgE levels, as shown in Fig. 4E–F. So far, we have completed the modification of the functionalized paper base for specific recognition of OVA-sIgE, and successfully established a working curve that can be used for visual quantitative analysis. By calculation, the minimum detection limits of the two working curves were 1.71 ng/ml (high OVA-sIgE levels) and 0.064 ng/ml (low OVA-sIgE levels), respectively. The clinical diagnostic threshold of ImmunoCAP for patients with food allergy was 0.84 ng/mL (0.35 KUA/L) (Cao et al., 2021). Therefore, our functionalized paper-based chips meet the requirements of clinical testing.

3.5. Design and fabrication of ISF-ICD

To achieve an integrated and user-friendly detection platform, a microfluidic chip was developed incorporating three key functional components: (1) a NP switch-controlled reagent delivery system, (2) functionalized paper-based detection substrates, and (3) minimally invasive microneedle ISF collectors. As illustrated in Fig. 5A and Fig. S4, the multilayer architecture employs distinct fluidic control mechanisms:

Pressure-Regulated Fluid Dynamics. The four-layer laminate structure (Pressure control layer → Reagent storage layer → capillarity layer → bottom layer) creates discrete microenvironments. Thermal bonding of polymeric layers establishes permanent fluidic channels while maintaining reagent stability. The NP switch mechanism (Fig. S5) generates localized negative pressure in PMMA-based reservoirs, preventing premature reagent flow through: $F = \Delta P \times A$. where ΔP represents the pressure differential and A the cross-sectional area of fluidic channels.

Capillary-Driven Sample Processing. ISF collected by GelMA MNs migrates vertically through the bottom layer's square apertures, then laterally along the paper substrate via capillary action. This two-phase transport ensures complete saturation of detection zones before reagent introduction.

Sequential Reagent Activation. Removal of the seal film from the designated NP switch initiates a controlled flow of reagent, with the pressure differential driving fluid forward at 8 mm/s. The staggered reservoir design enables temporally separated delivery of: **i)** Washing buffer (PBST); **ii)** Detection antibodies (anti-mouse OVA-sIgE antibody); **iii)** Chromogenic substrates. The fully assembled device (Fig. 5B) demonstrates reliable performance in simulated control reagent introduction and actual operation, with fluidic control validated by imaging (**GIF. S1**). The integrated ISF-ICD system overcomes critical point-of-care diagnostic challenges by enabling automated fluid handling to minimize user intervention, employing physical phase separation to prevent cross-contamination, and providing precise temporal control of multistep reactions.

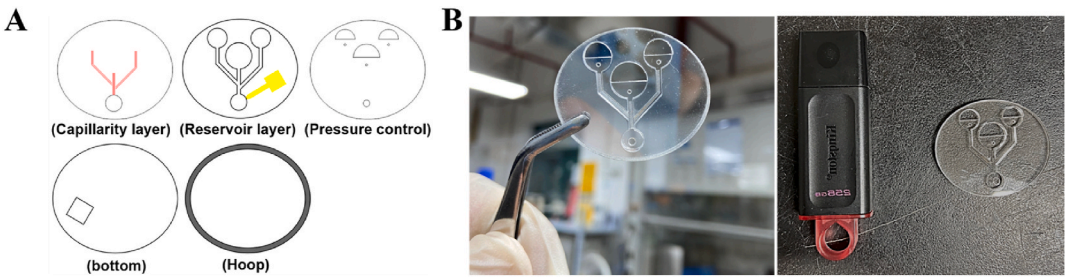


Fig. 5. Detailed design drawing of ISF-ICD **(A)** and assembled prototype photo **(B)**.

3.6. ISF-ICD in OVA-induced food allergy mouse models

We applied ISF-ICD to OVA food allergic mice to detect the content of OVA-sIgE in ISF of mice. However, simple tail vein injection of sIgE does not reflect the real process of allergy in animals. Therefore, we established a classic mouse OVA food allergy model (Fig. 6A) to more accurately and truly reflect the level of OVA-sIgE in food allergy mice, and to explore the dynamic relationship between serum OVA-sIgE and OVA-sIgE in ISF. With the increase in the number of oral OVA in mice, there was no significant change in the blank control group (Fig. S6A), and the allergic symptom score of OVA food allergy mice also gradually increased (Fig. S6C). After the fifth Intragastric, the blank control group had no significant change (Fig. S6B), while the OVA food allergy mice showed obvious diarrhea (Fig. S6D). This shows that we have successfully obtained OVA food allergy mice, which can be used for the next actual detection. The specific operation method is shown in Fig. 6B. The ISF-ICD is pressed onto the skin of depilated mice with a certain force, ensuring that the ISF-ICD is tightly attached to the mouse skin. After 15 min of ISF-ICD collection, a certain volume of ISF was transported to the detection area. HRP-anti-mouse OVA-sIgE was first controlled to enter the detection area for target recognition, then PBST was controlled to enter the detection area to remove excess antibodies and residual impurities, and finally TMB solution was controlled to enter the detection area for color development. The color results were taken by mobile phone and identified by RGB software. The content of OVA-sIgE in the ISF of the mouse was calculated to be about 294.1 ng/mL (Fig. 6C). In order to determine whether different detection sites have interference with the detection results, as shown in Fig. 6D, the ISF-ICD was used to detect the left, right, and middle of the back of the body of blank control mice (n = 3) and OVA food allergy mice (n = 7). In Fig. 6E, there was no significant difference in OVA-sIgE levels measured in different parts. In order to find out whether OVA-sIgE in ISF and OVA-sIgE in serum had the same dynamic change trend in time, we measured the serum OVA-sIgE and OVA-sIgE in ISF at 0 min to 24 h after oral administration of OVA in mice. The serum was detected by commercial ELISA kit, and ISF was detected by traditional blister method and ISF-ICD. As shown in Fig. 6F, the content of OVA-sIgE in the serum of allergic mice increased with time after oral administration of OVA, reaching the highest at 120

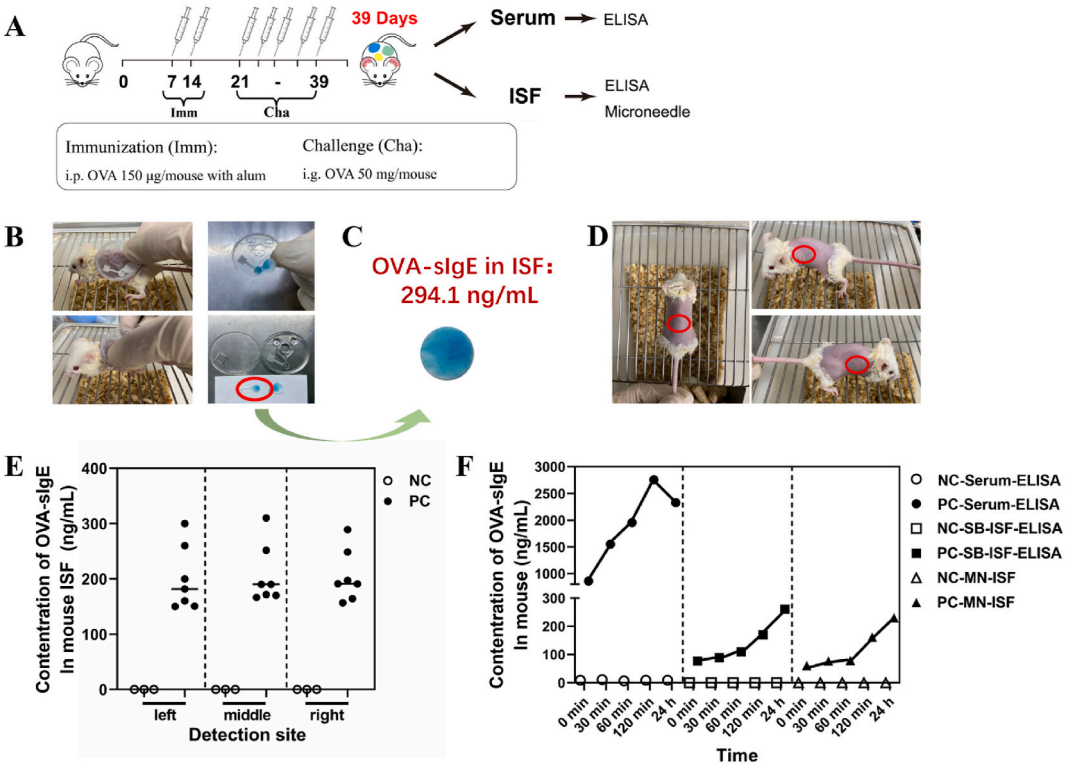


Fig. 6. (A) Immune process diagram of OVA food allergy mouse model. Practical application demonstration of the integrated ISF collection and detection device **(B)** and the quantitative results **(C)** of RGB analysis software. **(D)** schematic diagram of the microneedle invasion at different locations (the middle, left, and right sides of the mouse back). **(E)** OVA-sIgE levels in different parts of mice back. **(F)** Levels and dynamic changes of OVA-sIgE in serum or ISF of mice within 24 h after OVA challenge were analyzed by ELISA, suction blisters method (SB) and integrated ISF collection and detection device. 3 mice in the negative control (NC) group and 7 mice in the OVA food allergy group (positive control, PC) were analyzed.

min (2757.51 ± 22.15 ng/mL), and decreased after 24 h (2327.11 ± 29.58 ng/mL). It has been reported that this phenomenon is due to the short half-life of IgE in mice, which gradually increases after allergen stimulation, and IgE gradually decreases over time (Hirano et al., 1983; Infuhr et al., 2005; Shen and Stavnezer, 2001). The OVA-sIgE content measured by the blister method and the ISF-ICD at the same time after allergen stimulation was close, and gradually increased with time, but it was always lower than the serum OVA-sIgE concentration. At 30 min, the content of OVA-sIgE in serum was 1551.33 ± 30.51 ng/mL, but the OVA-sIgE in ISF measured by the two methods was 89.82 ± 11.26 ng/mL and 77.49 ± 9.11 ng/mL, respectively. The content of OVA-sIgE in ISF was lower than that in serum, about 1/15 of that in serum.

As the clinical use of skin patch test, skin prick test (Santos et al., 2023), etc., allergic reactions in the skin and dermis tend to be milder than the symptoms of oral excitation (Johansen et al., 2022; Wisgrill et al., 2021). For food allergy, it may be due to the fact that the specific IgE content in ISF is often low. Patients with food allergy often have symptoms of oral and respiratory allergies first, followed by skin allergies, which also gives the theoretical possibility that the content of sIgE in skin ISF is lower than that in serum (Breiteneder et al., 2020). At the same time, we also found that the growth trend of OVA-sIgE content in ISF is very similar to that of OVA-sIgE content in serum, but the half-life of sIgE in serum is shorter, while the sIgE in ISF can maintain a stable level for a longer period of time after allergen stimulation, which has a great advantage for allergen screening in some allergic patients who fail to see a doctor in time. Currently, there are few reports on the portable detection methods of OVA-sIgE or other allergen-specific antibodies in interstitial fluid. Compared with traditional ELISA, ImmunoCAP and NOVEOS systems, the ISF-ICD reported in this study demonstrates lower detection limits, reduced time consumption, simpler operation procedures, and minimal invasiveness (Table S2).

4. Conclusion

We integrated an ISF-ICD that can be used for painless detection of disease markers in ISF by using three modules: microneedles, functionalized paper-based, and NP switch -controlled microfluidic chips. With the help of HRP-TMB classical color reaction, the visual and portable detection of OVA-sIgE was realized. The ISF-ICD system demonstrated a minimum detection limit of 0.064 ng/mL for OVA-sIgE in ISF, with its measurements of OVA-sIgE content in OVA-allergic mice showing strong agreement with the blister method (77.49 ± 9.11 ng/mL vs. 89.82 ± 11.26 ng/mL at 30 min post-challenge). Notably, these ISF-based values were approximately 1/15 of the serum OVA-sIgE levels (1551.33 ± 30.51 ng/mL) quantified by ELISA.

These results highlight the ISF-ICD as a non-invasive and reliable alternative for allergen-specific IgE detection. Its capability to enable painless, real-time monitoring of allergic biomarkers positions it as a transformative tool for improving early diagnosis and personalized management of food allergies. Future studies should focus on validating its clinical applicability in human subjects.

CRediT authorship contribution statement

Jun Zhang: Writing – original draft, Validation, Software, Methodology, Formal analysis, Data curation, Conceptualization. **Huiting Lian:** Writing – review & editing, Validation, Data curation. **Guangming Liu:** Visualization, Data curation. **Qingmei Liu:** Visualization, Validation, Formal analysis. **Bin Liu:** Writing – review & editing, Supervision, Project administration, Funding acquisition. **Xiaofeng Wei:** Writing – review & editing, Supervision, Project administration, Funding acquisition.

Declaration of competing interest

The authors declare that they have no known competing financial interests or personal relationships that could have appeared to influence the work reported in this paper.

Acknowledgments

This study was supported by the National Natural Science Foundation of China (21904043, 21575044), the Natural Science Foundation of Fujian Province of China (2024J01085) and the Natural Science Foundation of Xiamen of China (3502Z202473051). Thank you for the scanning electron microscope of the Instrumental Analysis Center of Huaqiao University. We sincerely thank all the world 's silent struggle of medical personnel.

Appendix A. Supplementary data

Supplementary data to this article can be found online at https://doi.org/10.1016/j.bios.2025.117815.

Data availability

Data will be made available on request.

References

Bartha, I., Almulhem, N., Santos, A.F., 2024. Feast for thought: a comprehensive review of food allergy 2021-2023. J. Allergy Clin. Immunol. 153 (3), 576–594. https://doi.org/10.1016/j.jaci.2023.11.918.

Bigi, A., Cojazzi, G., Panzavolta, S., Roveri, N., Rubini, K., 2002. Stabilization of gelatin films by crosslinking with genipin. Biomaterials 23 (24), 4827–4832. https://doi.org/10.1016/S0142-9612(02)00235-1.

Bigi, A., Cojazzi, G., Panzavolta, S., Rubini, K., Roveri, N., 2001. Mechanical and thermal properties of gelatin films at different degrees of glutaraldehyde crosslinking. Biomaterials 22 (8), 763–768. https://doi.org/10.1016/S0142-9612(00)00236-2.

Boyd, H., Santos, A.F., 2025. Novel diagnostics in food allergy. J. Allergy Clin. Immunol. 155 (2), 275–285. https://doi.org/10.1016/j.jaci.2024.12.1071.

Breiteneder, H., Peng, Y.Q., Agache, I., Diamant, Z., Eiwegger, T., Fokkens, W.J., Traidl-Hoffmann, C., Nadeau, K., O'Hehir, R.E., O'Mahony, L., Pfaar, O., Torres, M.J., Wang, D.Y., Zhang, L., Akdis, C.A., 2020. Biomarkers for diagnosis and prediction of therapy responses in allergic diseases and asthma. Allergy 75 (12), 3039–3068. https://doi.org/10.1111/all.14582.

Cao, M., Han, X., Lu, C., Wang, Y., Xu, Z., Wang, S., Zhou, B., Zhang, C., Yu, C., Li, L., Wei, J.F., 2021. A novel method for precise detection of allergen-specific IgE via immobilizing his-tagged allergens to paper-based device. Allergy 76 (2), 567–571. https://doi.org/10.1111/all.14500.

Cao, N., Fu, Y., He, J., 2007. Mechanical properties of gelatin films cross-linked, respectively, by ferulic acid and tannin acid. Food Hydrocoll. 21 (4), 575–584. https://doi.org/10.1016/j.foodhyd.2006.07.001.

Dantzer, J.A., Kim, E.H., 2024. New approaches to food allergy immunotherapy. J. Allergy Clin. Immunol. Pract. 12 (3), 546–552. https://doi.org/10.1016/j.jaip.2023.10.018.

Eltayib, E., Brady, A.J., Caffarel-Salvador, E., Gonzalez-Vazquez, P., Zaid, A.A., McCarthy, H.O., McElnay, J.C., Donnelly, R.F., 2016. Hydrogel-forming microneedle arrays: potential for use in minimally-invasive lithium monitoring. Eur. J. Pharm. Biopharm. 102, 123–131. https://doi.org/10.1016/j.ejpb.2016.03.009.

Foong, R.X., Dantzer, J.A., Wood, R.A., Santos, A.F., 2021. Improving diagnostic accuracy in food allergy. J. Allergy Clin. Immunol. Pract. 9 (1), 71–80. https://doi.org/10.1016/j.jaip.2020.09.037.

Friedel, M., Thompson, I., Kasting, G., Polsky, R., Cunningham, D., Soh, H.T., Heikenfeld, J., 2023. Opportunities and challenges in the diagnostic utility of dermal interstitial fluid. Nat. Biomed. Eng. 7 (12), 1541–1555. https://doi.org/10.1038/s41551-022-00998-9.

Gupta, R.S., Warren, C.M., Smith, B.M., Blumenstock, J.A., Jiang, J., Davis, M.M., Nadeau, K.C., 2018. The public health impact of parent-reported childhood food allergies in the United States. Pediatrics 142 (6). https://doi.org/10.1542/peds.2018-1235.

Hirano, T., Hom, C., Ovary, Z., 1983. Half-life of murine IgE antibodies in the mouse. Int. Arch. Allergy Appl. Immunol. 71 (2), 182–184. https://doi.org/10.1159/000233385.

Infuhr, D., Crameri, R., Lamers, R., Achatz, G., 2005. Molecular and cellular targets of anti-IgE antibodies. Allergy 60 (8), 977–985. https://doi.org/10.1111/j.1398-9995.2005.00832.x.

Johansen, J.D., Bonefeld, C.M., Schwensen, J., Thyssen, J.P., Uter, W., 2022. Novel insights into contact dermatitis. J. Allergy Clin. Immunol. 149 (4), 1162–1171. https://doi.org/10.1016/j.jaci.2022.02.002.

Kolluru, C., Williams, M., Yeh, J.S., Noel, R.K., Knaack, J., Prausnitz, M.R., 2019. Monitoring drug pharmacokinetics and immunologic biomarkers in dermal interstitial fluid using a microneedle patch. Biomed. Microdevices 21 (1), 14. https://doi.org/10.1007/s10544-019-0363-3.

Li, J., Lu, H., Wang, Y., Yang, S., Zhang, Y., Wei, W., Qiao, Y., Dai, W., Ge, R., Dong, H., 2022. Interstitial fluid biomarkers' minimally invasive monitoring using microneedle sensor arrays. Anal. Chem. 94 (2), 968–974. https://doi.org/10.1021/acs.analchem.1c03827.

Li, J., Wei, M., Gao, B., 2024. A review of recent advances in microneedle-based sensing within the dermal ISF that could transform medical testing. ACS Sens. 9 (3), 1149–1161. https://doi.org/10.1021/acssensors.4c00142.

Lundberg, J., Rudling, M., Angelin, B., 2013. Interstitial fluid lipoproteins. Curr. Opin. Lipidol. 24 (4), 327–331. https://doi.org/10.1097/MOL.0b013e3283630846.

Min, J., Sempionatto, J.R., Teymourian, H., Wang, J., Gao, W., 2021. Wearable electrochemical biosensors in North America. Biosens. Bioelectron. 172, 112750. https://doi.org/10.1016/j.bios.2020.112750.

Popov, T.A., Passalacqua, G., Gonzalez-Diaz, S.N., Plavec, D., Braido, F., Garcia-Abujeta, J.L., Dubuske, L., Rouadi, P., Morais-Almeida, M., Bonini, S., Cheng, L., Ansotegui, I.J., 2020. Medical devices in allergy practice. World Allergy Organ. 13 (10), 100466. https://doi.org/10.1016/j.waojou.2020.100466.

Sampath, V., Abrams, E.M., Adlou, B., Akdis, C., Akdis, M., Brough, H.A., Chan, S., Chatchatee, P., Chinthrajah, R.S., Cocco, R.R., Deschildre, A., Eigenmann, P., Galvan, C., Gupta, R., Hossny, E., Koplin, J.J., Lack, G., Levin, M., Shek, L.P., Makela, M., Mendoza-Hernandez, D., Muraro, A., Papadopoulous, N.G., Pawankar, R., Perrett, K.P., Roberts, G., Sackesen, C., Sampson, H., Tang, M., Togias, A., Venter, C., Warren, C.M., Wheatley, L.M., Wong, G., Beyer, K., Nadeau, K. C., Renz, H., 2021. Food allergy across the globe. J. Allergy Clin. Immunol. 148 (6), 1347–1364. https://doi.org/10.1016/j.jaci.2021.10.018.

Santos, A.F., Riggioni, C., Agache, I., Akdis, C.A., Akdis, M., Alvarez-Perea, A., Alvaro-Lozano, M., Ballmer-Weber, B., Barni, S., Beyer, K., Bindslev-Jensen, C., Brough, H. A., Buyuktiryaki, B., Chu, D., Del, G.S., Dunn-Galvin, A., Eberlein, B., Ebisawa, M., Eigenmann, P., Eiwegger, T., Feeney, M., Fernandez-Rivas, M., Fisher, H.R., Fleischer, D.M., Giovannini, M., Gray, C., Hoffmann-Sommergruber, K., Halken, S., Hourihane, J.O., Jones, C.J., Jutel, M., Knol, E., Konstantinou, G.N., Lack, G., Lau, S., Marques, M.A., Marchisotto, M.J., Meyer, R., Mortz, C.G., Moya, B., Muraro, A., Nilsson, C., Lopes, D.O.L., O'Mahony, L., Papadopoulos, N.G., Perrett, K., Peters, R. L., Podesta, M., Poulsen, L.K., Roberts, G., Sampson, H.A., Schwarze, J., Smith, P., Tham, E.H., Untersmayr, E., Van Ree, R., Venter, C., Vickery, B.P., Vlieg-Boerstra, B., Werfel, T., Worm, M., Du Toit, G., Skypala, I., 2023. EAACI guidelines on the diagnosis of IgE-mediated food allergy. Allergy 78 (12), 3057–3076. https://doi.org/10.1111/all.15902.

Shen, C.H., Stavnezer, J., 2001. Activation of the mouse Ig germline epsilon promoter by IL-4 is dependent on AP-1 transcription factors. J. Immunol. 166 (1), 411–423. https://doi.org/10.4049/jimmunol.166.1.411.

Sicherer, S.H., Sampson, H.A., 2018. Food allergy: a review and update on epidemiology, pathogenesis, diagnosis, prevention, and management. J. Allergy Clin. Immunol. 141 (1), 41–58. https://doi.org/10.4049/jimmunol.166.1.411.

Takeuchi, K., Takama, N., Sharma, K., Paul, O., Ruther, P., Suga, T., Kim, B., 2022. Microfluidic chip connected to porous microneedle array for continuous ISF sampling. Drug Deliv. Transl. Re. 12 (2), 435–443. https://doi.org/10.1007/s13346-021-01050-0.

Tran, B.Q., Miller, P.R., Taylor, R.M., Boyd, G., Mach, P.M., Rosenzweig, C.N., Baca, J.T., Polsky, R., Glaros, T., 2018. Proteomic characterization of dermal interstitial fluid extracted using a novel microneedle-assisted technique. J. Proteome Res. 17 (1), 479–485. https://doi.org/10.1021/acs.jproteome.7b00642.

Wei, C., Fu, D., Ma, T., Chen, M., Wang, F., Chen, G., Wang, Z., 2024. Sensing patches for biomarker identification in skin-derived biofluids. Biosens. Bioelectron. 258, 116326. https://doi.org/10.1016/j.bios.2024.116326.

Wisgrill, L., Werner, P., Jalonen, E., Berger, A., Lauerma, A., Alenius, H., Fyhrquist, N., 2021. Integrative transcriptome analysis deciphers mechanisms of nickel contact dermatitis. Allergy 76 (3), 804–815. https://doi.org/10.1111/all.14519.

Yuan, A., Xia, F., Bian, Q., Wu, H., Gu, Y., Wang, T., Wang, R., Huang, L., Huang, Q., Rao, Y., Ling, D., Li, F., Gao, J., 2021. Ceria nanozyme-integrated microneedles reshape the perifollicular microenvironment for androgenetic alopecia treatment. ACS Nano 15 (8), 13759–13769. https://doi.org/10.1021/acsnano.1c05272.

Zhang, X., Zhou, C., Chen, T., Jiang, Z., Lu, C., Wu, C., Pan, X., Huang, Z., Peng, T., 2024. State-of-the-art strategies to enhance the mechanical properties of microneedles. Int. J. Pharm. (Amst.) 663, 124547. https://doi.org/10.1016/j.ijpharm.2024.124547.

Zhu, J., Zhou, X., Kim, H.J., Qu, M., Jiang, X., Lee, K., Ren, L., Wu, Q., Wang, C., Zhu, X., Tebon, P., Zhang, S., Lee, J., Ashammakhi, N., Ahadian, S., Dokmeci, M.R., Gu, Z., Sun, W., Khademhosseini, A., 2020. Gelatin methacryloyl microneedle patches for minimally invasive extraction of skin interstitial fluid. Small 16 (16), e1905910. https://doi.org/10.1002/smll.201905910.